

## Epitaxial Mn<sub>2.5</sub>Ga thin films with giant perpendicular magnetic anisotropy for spintronic devices

Feng Wu,<sup>1,a)</sup> Shigemi Mizukami,<sup>1</sup> Daisuke Watanabe,<sup>1</sup> Hiroshi Naganuma,<sup>2</sup> Mikihiro Oogane,<sup>2</sup> Yasuo Ando,<sup>2</sup> and Terunobu Miyazaki<sup>1</sup>

<sup>1</sup>WPI Advanced Institute for Materials Research, Tohoku University, 2-1-1 Katahira, 980-8577 Sendai, Japan

<sup>2</sup>Department of Applied Physics, Graduate School of Engineering, Tohoku University, 6-6-05 Aoba-yama, 980-8579 Sendai, Japan

(Received 13 February 2009; accepted 5 March 2009; published online 24 March 2009)

We report on epitaxial growth and magnetic properties of Mn<sub>2.5</sub>Ga thin films, which were deposited on Cr/MgO single crystal substrates by magnetron sputtering. X-ray diffraction results revealed the epitaxial relationships as Mn<sub>2.5</sub>Ga(001)[100]||Cr(001)[110]||MgO(001)[100]. The presence of (002) and (011) superlattice peaks indicates that the films were crystallized into DO<sub>22</sub> ordered structures. The perpendicular magnetic anisotropy (PMA) properties were found to be related to the extent of DO<sub>22</sub> chemical ordering. A giant PMA ( $K_u^{\text{eff}}=1.2 \times 10^7$  erg/cm<sup>3</sup>) and low saturation magnetization ( $M_s=250$  emu/cm<sup>3</sup>) can be obtained for the film with highest chemical ordering parameter ( $S=0.8$ ). © 2009 American Institute of Physics. [DOI: 10.1063/1.3108085]

Thin films with perpendicular magnetic anisotropy (PMA) are one type materials featured with easy magnetization axes perpendicular to the film surface. Since the discovery of PMA property in a Gd–Co amorphous film,<sup>1</sup> a variety of PMA films have been developed to overcome the superparamagnetic limit and enhance the thermal stability of ultrahigh-density magnetic storage devices.<sup>2–6</sup> Recently, research interest in applications of PMA films in the field of spintronics has increased remarkably. Spin valves<sup>7–9</sup> and magnetic tunneling junctions<sup>10–13</sup> with perpendicular anisotropy have been demonstrated to allow the realization of low-dimensional and highly reliable spintronic devices, e.g., spin-transfer switching magnetoresistive random access memory. Also, several physical phenomena including efficient electron spin injection into semiconductor from ferromagnetic contact in remanence<sup>14,15</sup> enhanced output signals in a spin-torque oscillator<sup>16</sup> and giant spin Hall effects<sup>17</sup> have been observed in spintronic devices made of PMA films.

For applications in spintronic devices, materials possessing large spin polarization ( $P$ ) and low saturation magnetization ( $M_s$ ) are strongly desired.<sup>7,18</sup> However, none of the present used PMA materials can satisfy this requirement. Mn<sub>*x*</sub>Ga ( $x=2–3$ ) with DO<sub>22</sub> crystal structure has the potential to possess such properties simultaneously according to previous theoretical and experimental results for polycrystalline alloys.<sup>19–23</sup> In this structure, an atomic layer of Mn and a layer containing both Mn and Ga atoms are arranged periodically along the  $c$ -axis [Figure 1(a)]. A potential high PMA property has been proposed by approximating the  $M$ - $H$  curves of polycrystalline alloy.<sup>19</sup> Classic neutron scattering experiments showed that this material had a ferrimagnetic structure and the magnetic moments of Mn atoms at sites I and II [Fig. 1(a)] were  $2.8 \pm 0.3 \mu_B$  and  $1.6 \pm 0.2 \mu_B$ , respectively. Consequently, a low  $M_s$  can be observed at room temperature although the Curie temperature is higher than 770 K.<sup>20</sup> The theoretically calculated spin polarization value as high as 88% at the Fermi level originates from the strong

difference in conductivity for minority and majority electrons,<sup>21</sup> which is a typical feature in type-III half metals.<sup>24</sup> To better comprehend the intrinsic properties of this material and realize its practical applications in spintronics, epitaxial Mn<sub>2.5</sub>Ga single crystal films are preferable, although they are still unavailable.

In this work, 100 nm thick Mn<sub>2.5</sub>Ga films were prepared on Cr-buffered MgO (001) single crystal substrates by a magnetron sputtering system with a base pressure of 10<sup>-6</sup> Pa. Detailed experimental procedure for the epitaxial Cr buffer layer can be found in the literature.<sup>25</sup> For Mn<sub>2.5</sub>Ga films, Ar pressure and sputtering power were set as 0.1 Pa and 25 W, respectively. The substrate temperature ( $T_s$ ) was varied from 250 to 500 °C. After deposition, the films were covered with a Ta layer of 2 nm for oxidation protection. The composition of the films was determined by an inductively coupled plasma mass spectrometer method. X-ray diffraction (XRD) patterns were measured by a high-resolution x-ray diffractometer (Bruker D8 Discover). The magnetization curves were measured at room temperature by a superconducting quantum interference device.

Figure 1(b) shows the XRD  $\theta$ - $2\theta$  patterns of the Mn<sub>2.5</sub>Ga films prepared at different  $T_s$ . In addition to peaks from MgO and Cr, only Mn<sub>2.5</sub>Ga (002) and (004) peaks can be observed, indicating that the Mn<sub>2.5</sub>Ga films were grown with the tetragonal  $c$  axis along the normal direction. The crystalline quality of the films was evaluated by full width at half maximum (FWHM) value of the (004) peak [Fig. 1(c)]. With  $T_s$  increasing from 250 to 400 °C, the FWHM decreases from 0.70° to 0.42°, suggesting the crystalline qualities of the Mn<sub>2.5</sub>Ga films be improved. However, the FWHM increases suddenly to 0.70° again when  $T_s$  changes to 450 °C and (004) peak shifts toward high angle in  $\theta$ - $2\theta$  pattern. We speculated this deterioration of crystalline quality originated from the diffusion of Cr buffer into the Mn<sub>2.5</sub>Ga films, although further study should be done to clarify this speculation. Since the XRD patterns of the DO<sub>22</sub> and  $L1_0$  crystal structure are quite similar,<sup>19,23</sup> it is impossible to differentiate between them using only  $\theta$ - $2\theta$  measure-

<sup>a)</sup>Electronic mail: fengwu@wpi-aimr.tohoku.ac.jp.

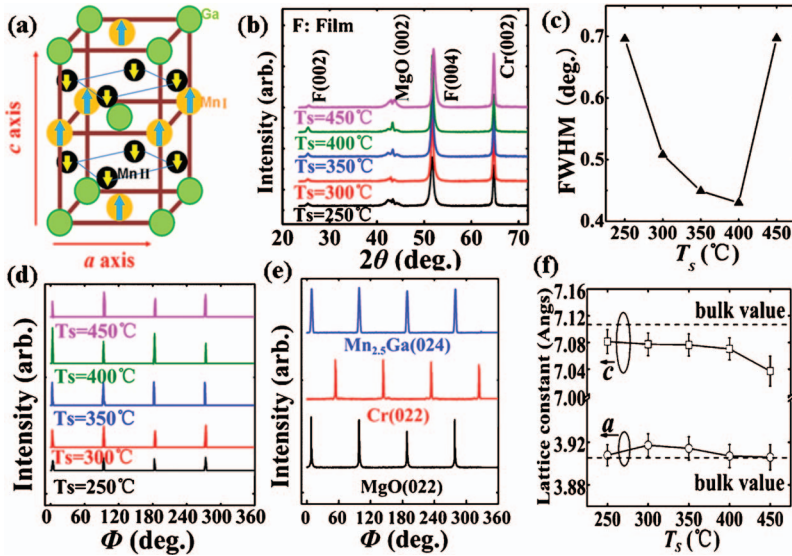


FIG. 1. (Color) (a) Schematic illustration of  $DO_{22}$  tetragonal crystal structure. The arrows in the Mn sites denote the direction of magnetization. (b) XRD  $\theta$ - $2\theta$  patterns and (c) FWHM of 004 peaks of films prepared at different  $T_s$ . (d) Pole figures of the (011) peaks for the  $Mn_{2.5}Ga$  films prepared at different  $T_s$ . (e) Pole figures of the  $Mn_{2.5}Ga/Cr/MgO$  heteroepitaxial structure in which the  $Mn_{2.5}Ga$  film was prepared at 400 °C. (f) The relationships between lattice constants and  $T_s$ .

ments for our films. Hence, pole figure measurements ( $\Phi$ -scan) were employed to confirm the crystal structure of the  $Mn_{2.5}Ga$  films. The presence of fourfold (011) peaks in all  $Mn_{2.5}Ga$  films clearly indicates that the films have crystallized into the  $DO_{22}$  structure because the (011) peak is a forbidden diffraction peak in the  $L1_0$  crystal structure [Fig. 1(d)]. To determine the epitaxial relationships between the  $Mn_{2.5}Ga$  films and Cr/MgO substrates, we measured the  $\Phi$ -scans of the MgO (022), Cr (022), and  $Mn_{2.5}Ga$  (024) peaks. A typical result for the film prepared at 400 °C is displayed in Fig. 1(e). The epitaxial relationship can be determined as  $Mn_{2.5}Ga(001)[100] \parallel Cr(001)[110] \parallel MgO(001) \times [100]$ , which also existed in the films prepared at other substrate temperatures. Lattice constants  $c$  and  $a$  for epitaxial  $Mn_{2.5}Ga$  films were plotted as a function of  $T_s$  in Fig. 1(f). The value of  $a$  is approximately equal to the bulk value while the value of  $c$  was found to be almost constant in the temperature region from 250 to 400 °C and smaller than the corresponding value for polycrystalline alloy.<sup>22</sup> Such deviation implies that tensile strain exists in the  $Mn_{2.5}Ga$  epitaxial

films because of lattice mismatch, which results from the different lattice spacing in  $Mn_{2.5}Ga$  [100] (3.909 Å) and Cr [110] (2.036 Å). When one lattice of  $Mn_{2.5}Ga$  matches two lattices of the Cr buffer, the lattice of  $Mn_{2.5}Ga$  would contract along the  $c$  axis.

The in-plane and out-of-plane  $M$ - $H$  curves of the film prepared at 400 °C are given in Fig. 2(a). A well-squared loop is observed for the out-of-plane  $M$ - $H$  curve. However, the in-plane  $M$ - $H$  curve exhibits almost zero remnant magnetization and cannot be saturated even under a magnetic field of 50 kOe. The results indicate that the easy axis of the magnetization is perpendicular to film plane. Also, this feature holds for the films prepared at other temperatures. The dependence of  $M_s$  on  $T_s$  for epitaxial  $Mn_{2.5}Ga$  films is shown in Fig. 2(b), where the value of  $M_s$  was obtained from the out-of-plane  $M$ - $H$  curve. From 250 to 300 °C, a sharp increase in  $M_s$  is observed. Further increase in  $T_s$  has a little effect on  $M_s$  and  $M_s$  stays at a nearly invariant value of 250  $emu/cm^3$ , which is larger or smaller than the bulk value.<sup>22,23</sup> For polycrystalline alloys, the  $M$ - $H$  curves cannot

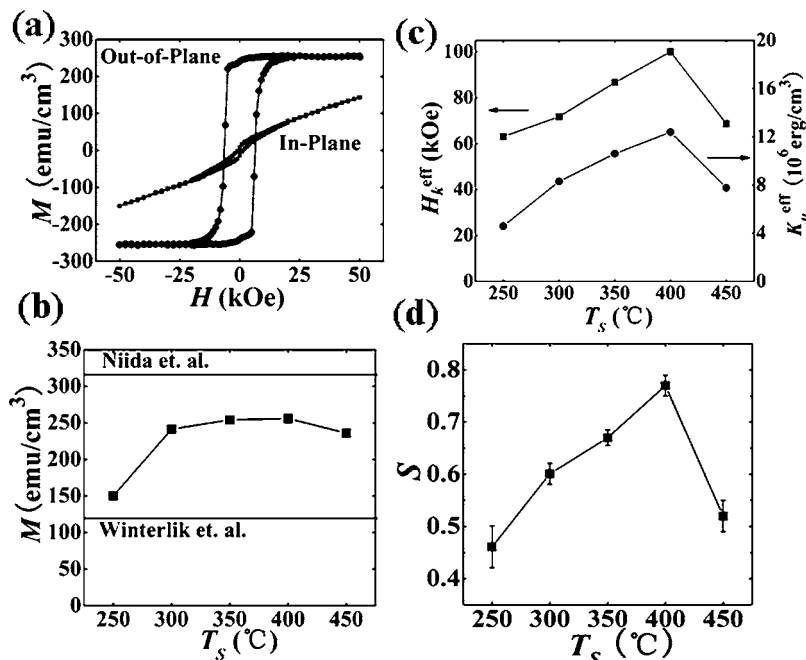


FIG. 2. (a) In-plane and out-of-plane  $M$ - $H$  curves of the epitaxial  $Mn_{2.5}Ga$  film prepared at 400 °C. (b) Saturation magnetization ( $M_s$ ) of films prepared at different  $T_s$ . (c) Dependence of effective anisotropic field ( $H_k^{eff}$ ) and anisotropic energy ( $K_u^{eff}$ ) on  $T_s$ . (d) The chemical ordering parameter ( $S$ ) at different  $T_s$ .

be saturated fully under a high magnetic field of 150 kOe, thus, such a difference between our films and those of polycrystalline alloys is not unusual. As mentioned above, obtaining a PMA material with low  $M_s$  is crucial for applications in spintronic devices. In this respect, our films are superior to the  $L1_0$ -ordered PMA films, like FePt (Refs. 4 and 9) and CoPt,<sup>13</sup> and can be comparable with the well-known ferrimagnetic PMA films, e.g., TbFeCo.<sup>10</sup>

To evaluate the PMA properties quantitatively, the effective magnetic anisotropy energy ( $K_u^{\text{eff}}$ ) was estimated using the relations  $K_u^{\text{eff}} = M_s H_k^{\text{eff}} / 2$ . Here, the effective anisotropy field ( $H_k^{\text{eff}}$ ) was defined as the extrapolated intersection of the in-plane  $M$ - $H$  curve with the saturation magnetization value of the out-of-plane  $M$ - $H$  curve. Figure 2(c) displays  $H_k^{\text{eff}}$  and  $K_u^{\text{eff}}$  versus  $T_s$ . With increasing  $T_s$ , both  $H_k^{\text{eff}}$  and  $K_u^{\text{eff}}$  increase monotonically and reach maximum values at 400 °C and then decrease with further increase in  $T_s$ . The highest  $K_u^{\text{eff}}$  value ( $1.2 \times 10^7$  erg/cm<sup>3</sup>) is comparable to that of other high PMA films, e.g., PtFe and CoFe.<sup>4,9,13</sup> Considering that the growth temperature of PMA films should be as low as possible for practical applications in spintronic devices, the epitaxial Mn<sub>2.5</sub>Ga film is very promising because high PMA can be obtained at relative low growth temperature.

The degree of chemical ordering as a parameter reflecting the probability of correct site occupation in the crystal structure often has significant influence on the final PMA property of the  $L1_0$ -ordered alloy film.<sup>4,13</sup> We investigated the degree of chemical ordering in the epitaxial Mn<sub>2.5</sub>Ga films to understand why PMA properties are enhanced with increasing  $T_s$ . In the DO<sub>22</sub> structure with a chemical formula of X<sub>3</sub>Y, the atom positions are (0,0,0) and (1/2,1/2,1/2) for Y atoms, (1/2,1/2,0) and (0,0,1/2) for X(I) atoms, and (0,1/2,1/4), (1/2,0,1/4), (0,1/2,3/4), and (1/2,0,3/4) for X(II) atoms. Reflection conditions for the DO<sub>22</sub> structure permit only reflection from the ( $hkl$ )-plane with the relationship of  $h+k+l=2n$  ( $h$ ,  $k$ , and  $l$ : Miller indices;  $n$ : integer). Fundamental and superlattice peaks can be determined from the structure factor  $F$  using a scattering factor for the atoms occupying each of sites  $f_Y$ ,  $f_{X(I)}$ , and  $f_{X(II)}$  as described below. When  $l$  is even and  $h$ ,  $k$ , and  $l/2$  are all even or all odd, i.e., (004) and (024), the structural factor for the fundamental peaks is  $F=2|f_{X(I)}+2f_{X(II)}+f_Y|$  and the intensities of these peaks are independent of the degree of order. On the other hand, when  $l$  is even and  $h$ ,  $k$ , and  $l/2$  are mixtures of even and odd, i.e., (002), the structural factor for superlattice peaks is  $F=2|f_{X(I)}+f_Y-2f_{X(II)}|$ , which is affected by the disorder between the Mn and Mn-Ga planes. When  $l$  is odd, i.e., (011), the structural factor for another superlattice peaks is  $F=2|f_{X(I)}-f_Y|$ , which decreases only by the preferential disorder between Y and X(I) atoms in the Mn-Ga planes. Based on the above guidelines, the (011) and (024) peaks were chosen as the superlattice and fundamental peak, respectively, to evaluate the ordering parameter ( $S$ ) using the equation of  $S = \sqrt{(I_{011}/I_{024})_{\text{meas}}/(I_{011}/I_{024})_{\text{calc}}}$ . Here,  $I_{011}$  and  $I_{024}$  are the integrated intensities of the (011) superlattice and (024) fundamental peak and  $(I_{011}/I_{024})_{\text{meas}}$  and  $(I_{011}/I_{024})_{\text{calc}}$  are the measured and calculated diffraction intensity ratios, respectively. We took into account the Lorentz-polarization factor, tem-

perature factor, absorption factor, multiplicity factor, etc. in the calculation of the ordering parameter  $S$ . As shown in Fig. 2(d), the change tendency of chemical ordering parameter ( $S$ ) with  $T_s$  is nearly the same as that of  $K_u^{\text{eff}}$  versus  $T_s$ . Thus, it can be considered that the enhancement of  $K_u^{\text{eff}}$  originates primarily from the improved chemical ordering in the DO<sub>22</sub> crystal structure.

In summary, we investigated the effects of substrate temperature on structural and magnetic properties of epitaxial Mn<sub>2.5</sub>Ga films. At optimum growth condition, the film exhibits giant PMA ( $K_u^{\text{eff}}=1.2 \times 10^7$  erg/cm<sup>3</sup>) and low saturation magnetization ( $M_s=250$  emu/cm<sup>3</sup>). Further experiments are being carried out to testify its high spin polarization.

This work was financially supported by NEDO ‘‘Spintronics Nonvolatile Devices Project.’’

- <sup>1</sup>P. Chaudhari, J. J. Cuomo, and R. J. Gambino, *IBM J. Res. Dev.* **17**, 66 (1973).
- <sup>2</sup>S. Iwasaki and K. Ouchi, *IEEE Trans. Magn.* **14**, 849 (1978).
- <sup>3</sup>P. F. Garcia, *J. Appl. Phys.* **63**, 5066 (1988).
- <sup>4</sup>T. Seki, T. Shima, K. Takanashi, Y. Takanashi, E. Matsubara, and K. Hono, *Appl. Phys. Lett.* **82**, 2461 (2003).
- <sup>5</sup>J. Sayama, K. Mizutani, T. Asahi, and T. Osaka, *Appl. Phys. Lett.* **85**, 5640 (2004).
- <sup>6</sup>S. N. Piramanayagam, *J. Appl. Phys.* **102**, 011301 (2007).
- <sup>7</sup>S. Mangin, D. Ravelosona, J. A. Katine, M. J. Carey, B. D. Terris, and E. E. Fullerton, *Nature Mater.* **5**, 210 (2006).
- <sup>8</sup>H. Meng and J. P. Wang, *Appl. Phys. Lett.* **88**, 172506 (2006).
- <sup>9</sup>T. Seki, S. Mitani, K. Yakushiji, and K. Takanashi, *Appl. Phys. Lett.* **88**, 172504 (2006).
- <sup>10</sup>N. Nishimura, T. Hirai, A. Koganei, T. Ikeda, K. Okano, Y. Sekiguchi, and Y. Osada, *J. Appl. Phys.* **91**, 5246 (2002).
- <sup>11</sup>J. H. Park, C. Park, T. Jeong, M. T. Moneck, N. T. Nufer, and J. G. Zhu, *J. Appl. Phys.* **103**, 07A917 (2008).
- <sup>12</sup>M. Nakayama, T. Kai, N. Shimomura, M. Amano, E. Kitagawa, T. Nagase, M. Yoshikawa, T. Kishi, S. Ikegawa, and H. Yoda, *J. Appl. Phys.* **103**, 07A710 (2008).
- <sup>13</sup>G. Kim, Y. Sakuraba, M. Oogane, Y. Ando, and T. Miyazaki, *Appl. Phys. Lett.* **92**, 172502 (2008).
- <sup>14</sup>N. C. Gerhardt, S. Hovel, C. Brenner, M. R. Hofmann, F. Y. Lo, D. Reuter, A. D. Wieck, E. Schuster, W. Keune, and K. Westerholt, *Appl. Phys. Lett.* **87**, 032502 (2005).
- <sup>15</sup>A. Sinsarp, T. Manago, F. Takano, and H. Akinaga, *Jpn. J. Appl. Phys., Part 2* **46**, L4 (2007).
- <sup>16</sup>D. Houssameddine, U. Ebels, B. Delaet, B. Rodmacq, I. Firastrau, F. Ponthier, M. Brunet, C. Thirion, J. P. Michel, L. Prejbeanu-Buda, M. C. Cyrille, O. Redon, and B. Dieny, *Nature Mater.* **6**, 447 (2007).
- <sup>17</sup>T. Seki, Y. Hasegawa, S. Mitani, S. Takahashi, H. Imamura, S. Maekawa, J. Nitta, and K. Takanashi, *Nature Mater.* **7**, 125 (2008).
- <sup>18</sup>K. Yagami, A. A. Tulapurkar, A. Fukushima, and Y. Suzuki, *Appl. Phys. Lett.* **85**, 5634 (2004).
- <sup>19</sup>H. Masumoto, K. Watanabe, and M. Mitera, *J. Jpn. Inst. Met.* **42**, 474 (1978).
- <sup>20</sup>E. Krón and G. Kádár, *Solid State Commun.* **8**, 1653 (1970).
- <sup>21</sup>B. Balke, G. H. Fecher, J. Winterlik, and C. Felser, *Appl. Phys. Lett.* **90**, 152504 (2007).
- <sup>22</sup>J. Winterlik, B. Balke, G. H. Fecher, and C. Felser, *Phys. Rev. B* **77**, 054406 (2008).
- <sup>23</sup>H. Niida, T. Hori, H. Onodera, Y. Yamaguchi, and Y. Nakagawa, *J. Appl. Phys.* **79**, 5946 (1996).
- <sup>24</sup>J. M. D. Coey, M. Venkatesan, and M. A. Bari, in *Lecture Notes in Physics*, edited by C. Berthier, L. P. Levy, and G. Martinez (Springer, New York, 2002), Vol. 595, pp. 377–396.
- <sup>25</sup>Y. Sakuraba, J. Nakata, M. Oogane, H. Kubota, Y. Ando, A. Sakuma, and T. Miyazaki, *Jpn. J. Appl. Phys.* **44**, 6535 (2005).